
**Separation Science and Technology**
Publication details, including instructions for authors and subscription information:
http://www.informaworld.com/smpp/title~content=t713708471

# Synthesis and Characterization of Molecularly Imprinted Polymers for Chromatographic Separations

Xiaolin Wei[a]; Azadeh Samadi[a]; Scott M. Husson[a]
[a] Department of Chemical Engineering, Clemson University, Clemson, SC, USA

**To cite this Article** Wei, Xiaolin , Samadi, Azadeh and Husson, Scott M.(2005) 'Synthesis and Characterization of Molecularly Imprinted Polymers for Chromatographic Separations', Separation Science and Technology, 40: 1, 109 — 129
**To link to this Article: DOI:** 10.1081/SS-200041880
**URL:** http://dx.doi.org/10.1081/SS-200041880

*Separation Science and Technology*, 40: 109–129, 2005

ISSN 0149-6395 print/1520-5754 online
DOI: 10.1081/SS-200041880

# Synthesis and Characterization of Molecularly Imprinted Polymers for Chromatographic Separations

**Xiaolin Wei, Azadeh Samadi, and Scott M. Husson**
Department of Chemical Engineering, Clemson University, Clemson, SC, USA



**Abstract:** The primary objective of this investigation was to discover the optimum solution-phase synthesis conditions for preparing molecularly imprinted polymers (MIPs) against Boc-L-Trp using a binary monomer system. Methacrylic acid (MAA) and 2-vinylpyridine (2-Vpy) were used as the two functional monomers with ethylene glycol dimethacrylate (EGDMA) as the cross-linker. Polymers prepared from two monomers showed improved binding strength and recognition capabilities compared to polymers that were prepared using a single monomer. The synergistic effect on binding was most pronounced for polymers prepared from a starting MAA : 2-Vpy molar ratio of about 1 : 5. A correlation was developed based on molecular interaction scales to relate the template-MIP binding strength to MIP composition. This correlation provides insights on the most important interaction types for the system studied; it also provides an explanation for the improved binding seen with a mixed monomer system. Polymerization temperature and cross-linking density were also investigated for their effects on the MIP recognition properties.

## INTRODUCTION

Stationary phase materials for affinity chromatography function by exploiting a selective interaction between a surface-bound ligand and a target ligate in solution (1, 2). Oftentimes, for a material to work successfully, it must

The authors thank the National Science Foundation for financial support of this work under grant number CTS-9983737.

Address correspondence to Scott M. Husson, Department of Chemical Engineering, Clemson University, Clemson, South Carolina, USA. E-mail: shusson@clemson.edu

differentiate among a number of chemically similar solutes in solution and specifically interact noncovalently with the target solute. Because of the need for specificity, most affinity stationary phase materials comprise a naturally occurring or biologically derived ligand anchored onto a solid support (3, 4). While such materials provide the requisite specificity, they suffer from a limited range of processing conditions (e.g., temperature and pH and high costs associated with production and/or isolation of the ligand). As a result, there exists broad interest in designing and fabricating synthetic affinity receptors that mimic the recognition properties of biological systems. One intriguing synthesis route involves a technique known as molecular imprinting.

Molecular imprinting is a templating technique that is used to produce physically and chemically selective binding sites in a polymer matrix. In this method, a cross-linked polymer is formed around the template. A high percentage of cross-linker is used to form rigid and insoluble polymers. After the template is extracted, imprint cavities remain in the polymer with functional groups that are capable of specific interaction with the template. These sites complement the template molecule in size, shape, and position of interacting functionalities. Consequently, they recognize the template and exhibit template-selective binding as measured, for example, by batch adsorption and chromatography experiments). Potential applications have been reported (5–8) for such materials and include the development of tailormade separation materials, antibody and receptor binding site mimics in recognition and assay systems, enzyme site mimics for catalysis, and recognition elements in chemical and biochemical sensors. Of particular relevance to the present contribution, molecularly imprinted polymers (MIPs) have shown promise as stationary phase materials for enantiomeric bioseparations.

A number of researchers have summarized the factors that contribute to the recognition properties of molecularly imprinted polymers (9–11); these factors include monomer functionalities, cross-linking functionalities and densities, solvents, and temperature. The arrangement of the monomers around the template molecule can be done via covalent interactions or by noncovalent interactions such as ionic interactions (12), hydrogen bonds (13), $\pi-\pi$ interactions (14), hydrophobic interactions (15), and metal chelation (16). Most studies on molecular imprinting employ one monomer and one cross-linking agent to exploit primarily one of these types of interactions. However, there are examples in the literature (17, 18), where improved binding sites result from interactions between a template molecule and two or more monomers. Some researchers have demonstrated that polymers prepared from two monomers show improved recognition capabilities compared to polymers that were prepared using the single monomers alone. One example is the work of Ramstrom et al. (17), who studied dansyl-L-phenylalanine as the template molecule and methacrylic acid (MAA) and 2-vinylpyridine (2-Vpy) as the functional monomers. An interesting result

was that a 1 : 1 monomer molar ratio gave enhanced performance over the single monomer materials.

This synergistic effect seems logical since each monomer contributes to the overall imprinting by interactions with different groups on the template. Given the structure of boc-L-tryptophan (Boc-L-Trp), with a carboxylic acid group, an indole group, and an amide linkage, it also seems logical that adjusting the 2-Vpy : MAA molar ratio may lead to an optimized material for this template. Therefore, the primary goal of this research was to test this hypothesis by synthesizing MIPs for Boc-L-Trp and characterizing their performance as chromatographic stationary phase materials. Further, a correlation was developed based on common molecular interaction scales to relate the strength of binding of the template with the functional monomer molar composition of the MIP materials.

## EXPERIMENTAL

### Materials

MAA (99%), 2-Vpy (97%) and ethylene glycol dimethacrylate (EGDMA, 98%) were obtained from Aldrich and purified by distillation under vacuum at 25 mm Hg prior to use. 2,2′-Azobis(isobutyronitrile) (AIBN, 98%) was purchased from Aldrich and used as received. Acetonitrile, methanol, and acetone were purchased as HPLC grade from Aldrich and used as received. Boc-L-Trp and Boc-D-Trp (99.8%) were purchased from Aldrich and Indofine Chemical Company, Inc. (Hillsborough, NJ, USA), respectively.



### Methods

#### Preparation of MIP

The MIPs were prepared by a conventional solution polymerization method that uses a common initiator, AIBN, that can be activated by thermal decomposition at 60°C and by UV irradiation (365 nm) at 4°C. MAA and 2-Vpy were used as the monomers and EGDMA as the cross-linking agent; acetonitrile was the solvent.

A typical reaction procedure follows to prepare the MIP: 152 mg (0.5 mmol) of Boc-L-Trp was dissolved in a mixture of 315 mg (3 mmol) of 2-Vpy, 258 mg (3 mmol) of MAA, 3964 mg (20 mmol) of EGDMA, 3 mL of acetonitrile, and 34 mg (0.2 mmol) of AIBN. The solution was sonicated for 5 min and sparged with nitrogen for 5 min, and then polymerized at 60°C or at 4°C under 365 nm UV light for 24h. The UV lamp (Model ENF-260C, 115 volts, 60 Hz and 0.20 amps) was from Spectronics Corporation. For UV

initiation, precautions were taken to provide a high surface-to-volume ratio for the polymerization solution; this precaution helps to provide uniform exposure to the UV radiation. Following polymerization, the bulk polymer was dried overnight under vacuum at 25 mm Hg and 50°C. Next, it was ground with a mortar and pestle and sieved between 200-mesh and 400-mesh screens to give particles with size dimensions between 38 μm and 75 μm. Fines were removed by sedimentation from ethanol; this step ensured that when the particles were packed in the column, no fines were available to block the pores in the frit of the column. The template and unreacted monomers and cross linker were extracted out by Soxhlet extraction for 12h using methanol as the solvent. Finally, the particles were dried under vacuum at 25 mm Hg and 50°C for 15 min. A similar procedure with no added template was used to prepare nonimprinted polymers (NIPs) as control materials. Nitrogen BET analysis showed that the specific surface areas were $7.6671 \pm 0.1269\,m^2/g$ for the MIPs and $13.9197 \pm 0.2632\,m^2/g$ for the NIPs, respectively.



## Batch Adsorption Studies

Known masses (typically 0.03 g) of MIP or NIP particles were contacted with known volumes (typically 5 mL) of Boc-L-Trp or Boc-D-Trp solutions in acetonitrile with initial concentrations ranging from 0.5 to 10.0 mmol/L. The samples were placed in a constant-temperature, reciprocating shaker bath at 25°C and 80 rpm for 24 h. Results of an initial rate study showed that equilibrium was reached after 20 h. The initial and final Boc-Trp concentrations were determined by HPLC. The HPLC instrument (HP 1100) and the reverse-phase HPLC column (Zorbax SB-$C_{18}$, 75 × 4.6 mm) were from Hewlett Packard. The mobile phase comprised 99.9% acetonitrile and 0.1% acetic acid by volume and had a flow rate of 1 mL/minute. Detection was performed by ultraviolet (UV) spectroscopy using a flow-through UV cell operating at 210 nm. The column temperature was 35°C.

## Curve Fitting of the Adsorption Isotherms

Three adsorption isotherm models were chosen to represent the experimental data. Model parameters were determined by nonlinear, least-squares regression of these data. Regression was done using the solver function in Microsoft Excel 2000 to minimize the standard error by varying the model parameters. The standard error was calculated as $(B_{exp} - B_{cal})^2$, where B represents the adsorption uptake of Boc-Trp in μmol/g polymer.

## Chromatography Column Preparations and Operating Conditions

A known mass (approximately 0.60 g) of the MIP or NIP particles (38–75 μm) was slurry packed into a blank column (Supelco; 25-cm × 2.1-mm ID).

This packed column was installed in the modular HPLC system for the capacity factor analyses of Boc-L-Trp from acetonitrile solution. The concentration of the test solution was 8 mmol/L, and the injection volume was 5 μL. For each test polymer, Boc-Trp retention time was measured; acetone was used as a reference compound, and its retention time was measured in a separate injection. The column chamber was maintained at 35°C by a column heater; temperature control was done by a PC using HP Chemstation software. The mobile phase comprised 99.9% acetonitrile and 0.1% acetic acid by volume and had a flow rate of 0.2 mL/minute. Detection was performed by ultraviolet (UV) spectroscopy using a flow-through UV cell operating at 210 nm.

## RESULTS AND DISCUSSION

### Batch Adsorption Studies



Strong binding site heterogeneity is a feature inherent to molecularly imprinted polymers. During the polymerization, not all template molecules form isolated complexes with the functional monomers (i.e., aggregates of the template molecule also form cavities) (18). In addition, even for isolated template molecules, they may interact with functional monomers with different stoichiometries (9). Some authors have reported that the process of grinding the polymer after polymerization can damage some imprinted sites; also, a significant fraction of imprints shrink after the template molecules are removed with polar organic solvents (20). Finally, it has been found that two types of pores are created in the polymer matrix during a typical polymerization (21): micropores with dimensions smaller than 20 Å and meso- and macropores with dimensions between 20 and 2000 Å. Both types of pores contain molecularly imprinted cavities.

Because of the site heterogeneity, these materials have binding sites with different binding affinities and selectivities. Therefore, the binding behavior of MIPs should be described using a heterogeneous adsorption model. Umpleby et al. (22) and Turiel et al. (23) have compared the Langmuir, Freundlich, and Langmuir-Freundlich (LF) models; and they have shown that the LF model provides a better fit to the experimental adsorption isotherms of MIPs than the other models. This result is partly due to the fact that the Langmuir and Freundlich models contain two parameters, while the LF model contains three parameters. The LF isotherm [Eq. (1)] describes the relationship between the equilibrium concentration of bound (B) solute and free (F) solute in solution with three coefficients

$$B = \frac{N_t a F^m}{1 + a F^m} \tag{1}$$

where m is the heterogeneity index, $N_t$ is the binding capacity (moles solute/mass polymer) in the polymer matrix, and $a$ is related to the median binding affinity constant ($K_0$) via $K_0 = a^{1/m}$. For a homogeneous system, where $m = 1$, the LF isotherm reduces to the Langmuir isotherm. The LF isotherm reduces to the Freundlich isotherm when either $a$ or F approaches zero.

Figure 1 presents the experimental adsorption isotherm data (symbols) for batch rebinding of Boc-L-Trp template on MIP and NIP prepared with 8 : 4 : 40 molar ratios of 2-Vpy:MAA : EGDMA. For the MIP, a 1 : 12 ratio was used of template to functional monomer (2-Vpy + MAA). The adsorption of Boc-L-Trp on NIP was considered to be nonspecific, and it was used as a control for comparison against the corresponding MIP. Figure 1 also shows adsorption data for Boc-D-Trp on the same MIP and NIP materials. Comparison of these data with those for Boc-L-Trp demonstrate that the MIP binds Boc-L-Trp specifically over its enantiomer. Because the Boc-D-Trp isotherm for adsorption onto the MIP lies slightly above that for the NIP, there may be some cross-reactivity of the imprint sites for the enantiomer. In both sets of data, the solute uptake, B, was considered to occur through surface attachment; it was calculated by the expression for composite uptake (24)

$$B = \frac{(F_i - F) \cdot V}{m} \tag{2}$$

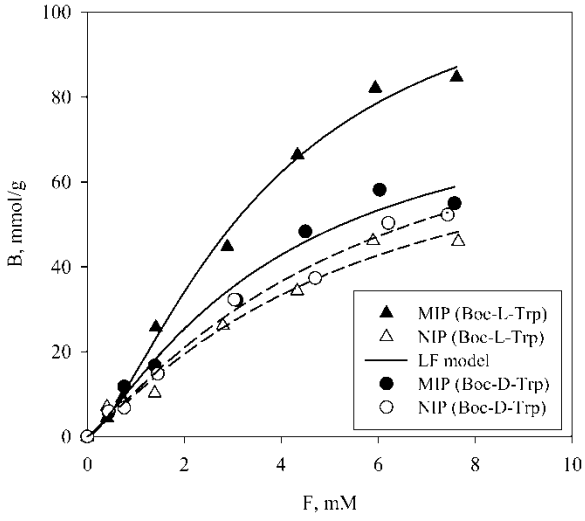


***Figure 1.*** Experimental adsorption isotherms of Boc-L-Trp and Boc-D-Trp for MIP (1 : 8 : 4 : 40) and NIP (0 : 8 : 4 : 40) at 25°C. The experimental data are shown with fits to the Langmuir–Freundlich adsorption model (curves).

where $F_i$ and F are the initial and final concentration of Boc-L-Trp or Boc-D-Trp solutions, respectively; V is the volume of Boc-L-Trp solution, and m is the mass of the polymer.

The curves on Fig. 1 represent the model fits to the experimental MIP and NIP adsorption data using the LF binding model. Table 1 gives the model coefficients obtained from nonlinear regression. For both MIP and NIP, the LF model gave slightly better fits to the experimental isotherms than did the Langmuir or Freundlich models. For the MIP, the values for $(B_{exp} - B_{cal})^2$ were 103.7, 202.2, and 41.2 $(\mu mol/g)^2$ for the Langmuir, Freundlich, and LF fits. For the NIP, the values were 47.8, 64.4, and 45.9 $(\mu mol/g)^2$, respectively. For the NIP, the deviation values for the Langmuir and LF models were similar. This result is not surprising since the factors that lead to site heterogeneity in MIPs are not at play in the preparation of NIPs.

Prior to the preparation of the imprinted polymers, the maximum number of specific binding sites for the MIP was estimated to be $110\,\mu mol/g$ assuming that all the added template molecules can form binding sites. The actual number of specific binding sites $[N_t(MIP) - N_t(NIP)]$ was determined to be about $35.8\,\mu mol/g$ from the LF isotherm, much lower than the estimated value. This discrepancy might be due to several factors: Some of the binding sites were embedded and not available for rebinding, some were destroyed during the grinding process, or some aggregate binding sites (imprints formed by multimers of template) were present in the polymer matrix.



***Table 1.*** Fitted parameters for the Langmuir, Freundlich, and LF determined by regression of the MIP and NIP adsorption isotherm data

| | Boc-L-Trp | | Boc-D-Trp | |
|---|---|---|---|---|
| Fitting coefficient | MIP | NIP | MIP | NIP |
| Langmuir–Freundlich | | | | |
| $N_t$ ($\mu mol/g$) | 116.2 | 80.4 | 97.5 | 91.5 |
| a $(mM)^{-m}$ | 0.148 | 0.142 | 0.153 | 0.132 |
| m | 1.478 | 1.158 | 1.155 | 1.163 |
| $K_0$ $(mM^{-1}) = a^{1/m}$ | 0.275 | 0.186 | 0.197 | 0.176 |
| Freundlich | | | | |
| $N_t a$ $(\mu mol/g \cdot mM^m)$ | 19.44 | 11.62 | 15.1 | 12.0 |
| m | 0.767 | 0.717 | 0.696 | 0.756 |
| Langmuir | | | | |
| $N_t$ ($\mu mol/g$) | 206.6 | 103.6 | 116.3 | 125.0 |
| a $(mM^{-1})$ | 0.100 | 0.116 | 0.139 | 0.100 |

## Chromatography Studies

The binding characteristics of MIPs and NIPs were compared on the basis of capacity factor. Capacity factor is one measure of the binding strength of a compound to the stationary phase material; the higher its value, the more strongly the compound is retained on the stationary phase. By definition, capacity factor is

$$k' = \frac{t_R - t_0}{t_0} \tag{3}$$

where $t_R$ is the retention time of the template compound, and $t_0$ is the retention time of a reference compound. In this study, acetone was chosen as the reference compound.

Three factors were studied that impact the MIP recognition properties, and, thus, the capacity factors: the polymerization temperature, the molar ratio of functional monomers, and the molar ratio of functional monomers to cross-linker.

### The Effect of Polymerization Temperature on Capacity Factor

Intermolecular interactions between the template and functional monomers depend strongly on temperature. So it is believed that the polymerization temperature should play an important role on imprint formation; stronger specific interactions should lead to more, well-formed imprint sites.

Table 2 shows capacity factor results for two MIPs that were made at two different temperatures: Polymer A was made at 4°C under UV irradiation; its capacity factor for Boc-L-Trp was 2.097 for the conditions used. Polymer B was made at 60°C; its capacity factor was 0.351 for the same chromatography conditions. The capacity factor increased dramatically as the synthesis temperature was decreased. At lower temperatures, template molecules interact more strongly with the functional monomers. The result is more,

***Table 2.*** Effect of polymerization temperature on capacity factor for imprinting of Boc-L-Trp. Functional monomers were methacrylic acid and 2-vinyl pyridine

| Polymer | Functional monomers | Retention time (min) | | Capacity factor of Boc-L-Trp |
|---|---|---|---|---|
| | | Acetone | Boc-L-Trp | |
| **A** : 1 : 8 : 8 : 40[a] (4°C, 365 nm) | 2-Vpy/MAA | 2.689 | 8.327 | 2.097 |
| **B** : 1 : 8 : 8 : 40[a] (60°C) | 2-Vpy/MAA | 2.942 | 3.976 | 0.351 |

[a]The molar composition of print molecule to 2-Vpy to MAA to EGDMA.

well-formed complexes that result in more binding sites in the product MIP. This result is consistent with other literature (25) on the effect of synthesis temperature on imprint formation. For all subsequent studies, UV irradiation at 4°C was used to initiate polymerization.

## The Effect of Functional Monomer Composition on Capacity Factor

Two different monomers were employed to make a set of polymers; one was methacrylic acid (MAA); the other was 2-vinylpyridine (2-Vpy). Based on the different chemical structures and physical properties of these two monomers, the interactions between the template molecule and individual monomers are different. For example, Moller et al. (26) has reported that MIPs prepared using the basic monomer (2-Vpy) had much stronger recognition ability for acidic templates than the acidic monomer (MAA). In order to find the polymer with the strongest and most selective rebinding properties for the template, MIPs with different initial ratios of these monomers were prepared and characterized. Table 3 displays the initial compositions used, along with results of chromatography. In this set, the moles of template molecule and cross linker were fixed, and the *total* number of moles of functional monomer was kept constant.

In order to understand why a mixed monomer system of MAA and 2-Vpy provided enhanced binding of this template, an attempt was made to correlate strength of binding (as measured by capacity factors) with the molecular interaction properties of the monomers and template using Abraham's

***Table 3.*** Capacity factor data for Boc-L-Trp on MIP and NIP materials differing in composition

| Polymer composition | Type of polymer | Capacity factor |
|---|---|---|
| 1 : 12 : 0 : 40 | MIP | 5.926 |
| 0 : 12 : 0 : 40 | NIP | 2.106 ± 0.163 |
| 1 : 11 : 1 : 40 | MIP | 8.105 ± 0.207 |
| 0 : 11 : 1 : 40 | NIP | 2.689 ± 0.075 |
| 1 : 9 : 3 : 40 | MIP | 6.594 |
| 0 : 9 : 3 : 40 | NIP | 1.980 |
| 1 : 8 : 4 : 40 | MIP | 7.281 ± 0.193 |
| 0 : 8 : 4 : 40 | NIP | 2.041 ± 0.021 |
| 1 : 6 : 6 : 40 | MIP | 4.824 ± 0.135 |
| 0 : 6 : 6 : 40 | NIP | 2.101 ± 0.340 |
| 1 : 4 : 8 : 40 | MIP | 1.882 ± 0.093 |
| 0 : 4 : 8 : 40 | NIP | 1.255 ± 0.062 |
| 1 : 0 : 12 : 40 | MIP | 0.218 |
| 0 : 0 : 12 : 40 | NIP | 0.210 |

hydrogen-bonding acidity and basicity scales (27, 28). The analysis that follows utilizes several simplifying assumptions that allow a qualitative assessment of binding: Firstly, the template is represented by three "groups," as shown in Table 4, and each group associates with only one functional monomer (MAA or 2-Vpy). (Implicit in this assumption is that the cross-linking agent serves only a role in forming the polymer matrix and does not participate in specific interactions with the template. Based on the template to functional monomer molar concentrations of 1 : 12 used experimentally, it is possible to saturate all template "groups" with functional monomer units.) In order to form an association complex, each monomer unit is first removed from the solvent. Thus, there is an energy penalty to break the monomer/solvent interactions prior to binding with the template. There is a similar energy penalty to break template/solvent interactions; however, since this contribution to the overall binding is independent of the monomer system, we do not formally include a separate term for it. For the mixed monomer systems, arrangement of the monomers with the three template "groups" is done in such a way to maximize the overall binding interactions. Consideration is given to hydrogen bonding interactions, dispersion interactions, and dipolar interactions according to Abraham's scales. Finally, only first coordination shell effects are considered, with the composition of this coordination shell assumed to be equal to the starting monomer composition. While second coordination shell effects have been shown to influence metal ion imprinting in the presence of a metal chelating agent (29, 30), it is not possible to experimentally decouple first and second coordination shell effects for our system, since the complexing agents that form the first coordination shell (MAA and 2-Vpy) also make up the polymer matrix (second coordination shell and beyond). For this reason, we choose to develop the correlation based on a measurable: the starting monomer composition.

The interaction values were used to correlate the capacity factor data in Table 3 for Boc-L-Trp on MIP materials made with different functional monomer compositions. Using the approach of Abraham, the following expression was used to correlate log k′ to molecular interactions:

$$\log k' = c + p\pi + r\mathbf{R} + a\mathbf{AB} \qquad (4)$$

where the terms p, r**R**, a**AB** represent specific net dipolar, dispersive, and hydrogen-bonding acid-base interactions between the monomer units and the template. The values of $\pi$, **R**, and **AB** depend on composition, since different monomer units have different interaction parameter magnitudes. The constants in Eq. (4) represent the tendency of the monomer units and the template to interact through dipolar, dispersive, and hydrogen-bonding acid-base interactions; they were fit by nonlinear regression to the experimental log k′ vs. mole fraction data. Table 4 compiles values for $\pi$, R, A, and B for

***Table 4.*** Interaction parameter values for the template functional groups, monomers, and solvent taken from Ref. (27)

| Group | R | $\pi$ | A | B | Comments |
|---|---|---|---|---|---|
| MAA | 0.265 | 0.67 | 0.61 | 0.52 | Approximated by adding $-C=CH_2$ structural unit to acetic acid[a] |
| 2-Vpy | 0.613 | 0.71 | 0.00 | 0.59 | Values used are for 2-ethyl-pyridine |
| Acetonitrile | 0.237 | 0.90 | 0.07 | 0.32 | |
| Template group 1 | 1.223 | 1.25 | 0.41 | 0.43 | Approximated by summation of benzene and pyrrole group constants |
| Template group 2 | 0.210 | 0.62 | 0.60 | 0.45 | |
| Template group 3 | 0.400 | 1.55 | 0.40 | 1.17 | Approximated by summation of n-methylacetamide and t-butyl ether group constants |

[a]Calculation done according to Ref. (28).

the monomers, solvent, and template "groups." The Appendix outlines the procedure used to calculate the composition dependent parameters, $\pi$, **R**, and **AB** for association of the template with a set of monomer units.

Figure 2a shows the experimental capacity factor data as symbols; the curve represents the correlation with the best-fit parameter values of $c = -19.20$, $p = 34.27$, $r = 1.88$, and $a = 0.98$. Figure 2b breaks down the contributions to log $k'$ in order to understand what interactions may be most important to template binding. From this analysis, it appears that dipolar interactions influence binding strongly compared to dispersive and hydrogen-bonding acid-base interactions for this system. The maximum seen in the capacity factor vs. mole fraction data can be interpreted in terms of competing importance of dispersive vs. hydrogen-bonding acid-base interactions; the former is a decreasing function of mole fraction of MAA, whereas the latter is an increasing function. The inset of Fig. 2b shows these competing contributions more clearly.

As an aside, this interaction analysis also lends itself to the study of template aggregation. For example, comparing the interactions of two isolated Boc-L-Trp with acetonitrile solvent against those for a template–template aggregate, one finds that template self-association in acetonitrile should be very favorable compared to isolated, fully solvated template molecules. This fact supports the notion that template aggregates are imprinted in addition to single template molecules.

For each polymer, the molar ratio between template molecule and total monomers was 1 : 12. In order to compare the imprint effect of these polymers, one must also consider the effect on retention time contributed by functionality on the NIPs. The enhancement factor, $k'_{MIP}/k'_{NIP}$, was used to compare the imprinting effect; Fig. 3 presents the results. From these experimental data, larger enhancement factors were observed for some mixed monomer systems than the corresponding single-monomer systems. Furthermore, there appears to be an optimum monomer composition with a 1 : 2 molar ratio of MAA : 2-Vpy that gives a maximum enhancement factor.

The difference in optimum monomer composition for maximizing strength of association and maximizing enhancement factor has implications in the design of MIP materials. For example, if the design aim was to make a material for concentrating this solute from solution (e.g., solid-phase extraction), one would elect to make an MIP with a 1 : 5 molar ratio of MAA : 2-Vpy. On the other hand, if the design aim was to separate Boc-L-Trp selectively from other solutes, then a 1 : 2 molar ratio would give the desired selectivity.

## The Effect of Monomer-to-cross-linker Ratio on Capacity Factor

The impact of total molar concentration of the functional monomers on the capacity factor was also studied. Table 5 shows the results; a higher functional monomer-to-cross-linker ratio resulted in a lower capacity factor. Yilmaz et al.

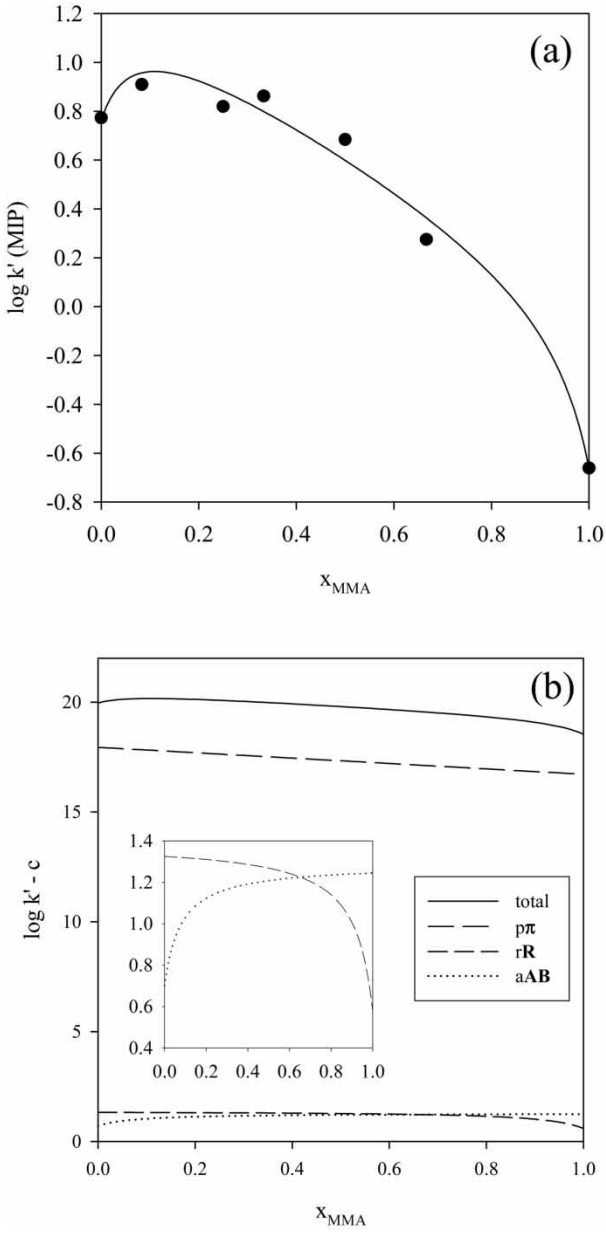


***Figure 2.*** Capacity factor data for Boc-L-Trp on MIP materials of differing MAA mole fraction. (a) Comparison of experimental data (symbols) with fitted correlation (curve). (b) Contributions to log k′ correlation resulting from dipolar (p$\boldsymbol{\pi}$), dispersive (r**R**), and hydrogen-bonding acid-base (a**AB**) interactions. Inset shows an expanded view of the dispersive and hydrogen-bonding acid-base interaction contributions.

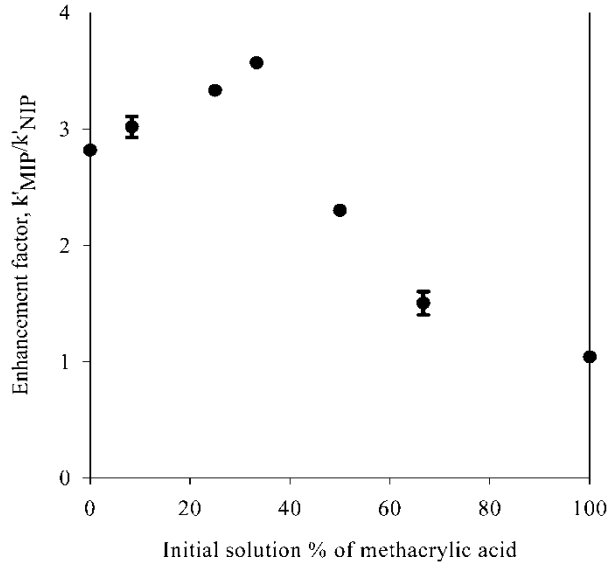


***Figure 3.*** The effect of initial molar percentage of MAA on enhancement factor. Percentages represent the molar percentage of functional monomer (MAA + 2-Vpy). Template was Boc-L-Trp. Polymerization was done at 4°C.

(31) has reported that an optimized degree of cross-linking exists in many imprinting systems. Two effects should be considered to explain this observation. Higher cross-linker percentages result in more rigid polymer frameworks. The more rigid framework often enhances the imprinting effect; the shape of the imprint cavities has less flexibility. Lower cross-linker percentages provide more functional monomer available for specific interactions with the template. For the polymers in this study, higher-quality imprints at higher cross-linker percentage imply that the number of monomer functionalities, even at low functional monomer percent, is sufficient to saturate the functional sites of the template. Therefore, in this case, the rigidity of the polymer is the most important factor that controls the imprinting effect.

***Table 5.*** The effect of changing the functional monomer-to-cross-linker ratio on capacity factor. Template was Boc-L-Trp. Polymerization was done at 4°C

| | Retention time (min) | | |
|---|---|---|---|
| Polymer composition | Acetone | Boc-L-Trp | Capacity factor |
| 1 : 8 : 8 : 40 | 2.689 | 8.237 | 2.097 |
| 1 : 6 : 6 : 40 | 2.879 | 17.166 | 4.962 |

The Effect of Mobile-phase Composition on Capacity Factor

The effect of the mobile-phase polarity on capacity factor was studied by changing its composition from 99.9% acetonitrile to mixtures of acetonitrile and water. By increasing the mole fraction of water, the polarity of the mobile phase was increased. Figure 4 shows that the retention time of the template molecule went through a minimum at a water composition of about 40 mol %. This observation may be related to the solvating power of acetonitrile-water mixtures for organic anions, such as amino acids, that have their maximum solvating power in the water mole fraction range 0.2–0.3 (32). This maximum of solvating power shifts the partitioning of Boc-L-Trp toward the mobile phase; consequently, the retention time decreases. The column behaves like a reverse-phase chromatography column because of the presence of the hydrophobic imprint cavity in the polymer matrix.



## Resolution of Enantiomers on the Boc-L-Trp-Imprinted Stationary Phase

The Boc-L-Trp-imprinted polymer with maximum selectivity (1 : 8 : 4 : 40) and the corresponding control polymer (0 : 8 : 4 : 40) were packed into

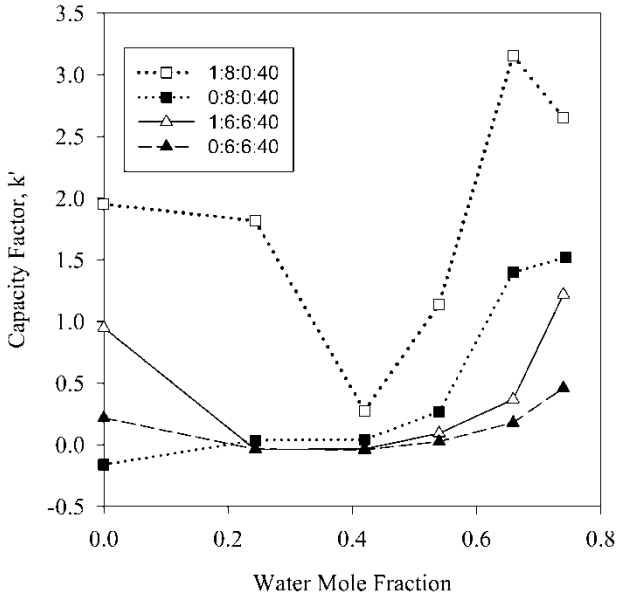


***Figure 4.*** Effect of the mobile phase composition on capacity factor. Water mole fractions are given for water/acetonitrile mixtures.

chromatography columns to perform the enantiomeric separation of Boc-L-Trp and Boc-D-Trp. Figure 5 shows two chromatograms that compare this separation on NIP and MIP. Since the peaks were not resolved fully on the 25 cm column, the samples of the enantiomers were injected onto the column individually. Figure 5A shows that no separation occurs for the enantiomers on the NIP material. In contrast, Fig. 5B shows that the retention time of Boc-L-Trp increased dramatically from 15.5 min to 22.5 min on the MIP, while there was no significant change of retention time for Boc-D-Trp. This result proved that some extent of resolution of the enantiomers was achieved by this imprinting technique, consistent with results from the batch adsorption studies. From Fig. 5B, a value of height equivalent to a theoretical plate was calculated to be 3.5 cm. A selectivity coefficient was determined to be $K_{DL} = 0.62$. Finally, the capacity factor for Boc-D-Trp was measured to be 2.97. With these values, the length of column needed to provide a resolution value of $R_s = 1$ (peaks resolved to 96%) was calculated to be 267 cm from

$$L = 16 \cdot R_s^2 \cdot H \cdot \left(\frac{K_{DL}}{K_{DL} - 1}\right)^2 \left(\frac{1 + k'_D}{k'_D}\right)^2 \quad (5)$$

Overcoming peak broadening would reduce this column length significantly. Improvements are possible by decreasing the size of the MIP particles; making more uniform, spherical particle shapes; improving the packing technique; and optimizing run conditions. Current efforts are focused on preparing ultrathin polymer films on uniform, solid support materials.



## CONCLUSIONS

Imprinted polymers were prepared for the protected amino acid, Boc-L-Trp, using a mixed monomer system of MAA and 2-Vpy. Experimental adsorption isotherms for these MIP materials and their corresponding nonimprinted polymers (NIPs) demonstrated that the MIPs had a higher binding capacity and affinity for Boc-L-Trp; all isotherms were described well by the Langmuir–Freundlich adsorption model. By changing the initial concentration of the two chemically distinct functional monomers, the results show that, over a range of compositions, MIPs produced with binary monomer systems had higher capacity factors and enhancement factors than the corresponding MIPs using a single monomer for the system studied. Alone, 2-Vpy produced a better MIP than MAA for Boc-L-Trp. This result and the maximum in the capacity factor vs. MIP composition were explained based on a correlation developed using common intermolecular interaction scales.

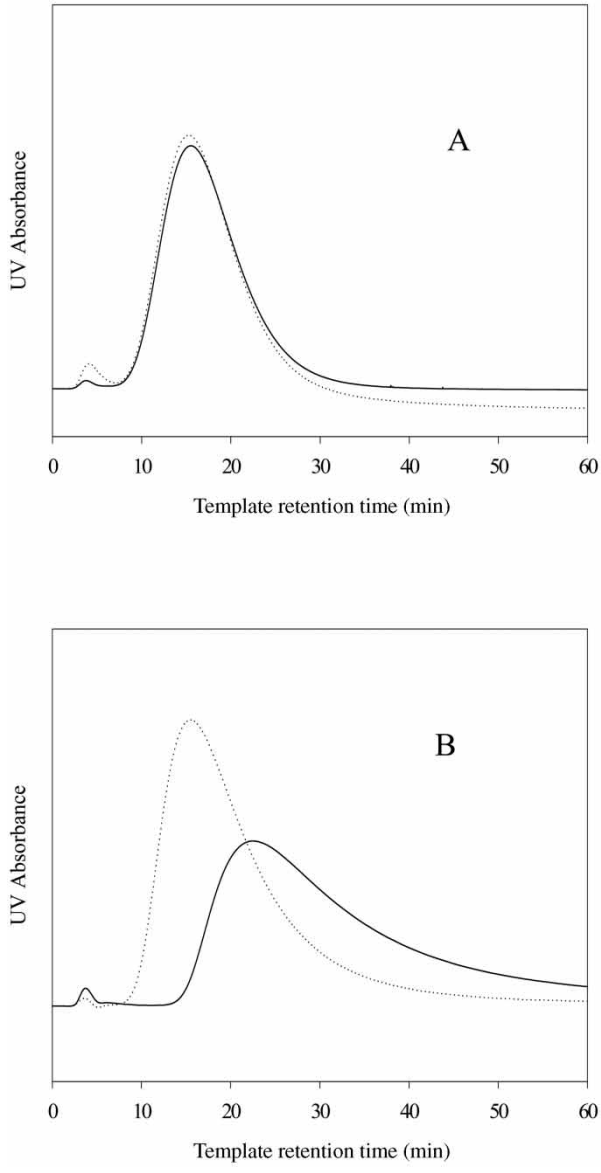


***Figure 5.*** Resolution of enantiomers on the Boc-L-Trp imprinted 2Vpy–EGDMA columns. Particles with a size between 37 μm and 75 μm were packed into 2.1 mm × 25 cm stainless steel column. Analyses were performed at 35°C under isocratic conditions using acetonitrile–acetic (99.9% : 0.1%, v/v) as the eluent at a flow rate of 0.2 mL/minute. Solid curves represent the peak of Boc-L-Trp and dotted curves represents the peak of Boc-D-Trp. (A): Separation on NIP (0 : 8 : 4 : 40) and (B): Separation on MIP (1 : 8 : 4 : 40).

## APPENDIX

The strength of association (measured as log k′) of a template molecule with three functional monomers was calculated to be the weighted summation of three types of interactions: dipolar, dispersive, and hydrogen-bonding acid base. The parameters that represent these interactions in Eq. (4) are $\pi$, **R**, and **AB**; they were evaluated by the procedure that follows. For illustrative purposes, calculation of these parameters will be done for the case where one template molecule forms an association complex with one MAA monomer unit and two 2-Vpy monomer units. Scheme A1 illustrates the association complex.

Each parameter in Eq. (4) represents the net strength of interaction according to

$$\pi = \pi(\text{Template} : \text{monomers}) - \pi(\text{Monomers} : \text{solvent}) \quad \text{(A1)}$$

$$\mathbf{R} = \mathbf{R}(\text{Template} : \text{monomers}) - \mathbf{R}(\text{Monomers} : \text{solvent}) \quad \text{(A2)}$$

$$\mathbf{AB} = \mathbf{AB}(\text{Template} : \text{monomers}) - \mathbf{AB}(\text{Monomers} : \text{solvent}) \quad \text{(A3)}$$

Evaluation of the strength of interaction between two groups is done by multiplying the individual group interaction parameters. For all hydrogen-bonding, acid-base interactions, the A parameter of the first group is multiplied by the B parameter of the second and vice versa.

Table A1 lists all relevant calculations for the template monomer association complex illustrated in Scheme A1. Notice that the calculated values depend on the composition of the complex through the number of MAA : 2-Vpy monomer units.

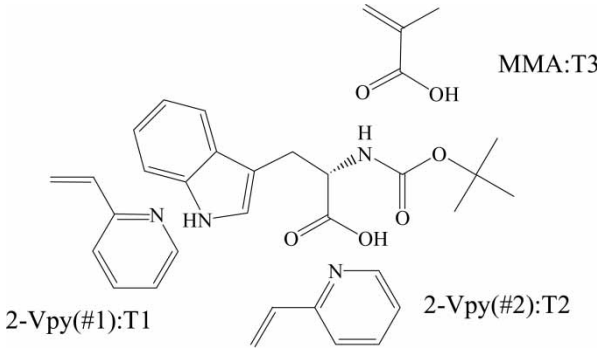


***Scheme A1.***

***Table A1.*** Calculation of interaction parameters for creation of an association complex between Boc-L-Trp, one MAA monomer unit, and two 2-Vpy monomer units

| Association groups | $\pi$ | **R** | **AB** |
|---|---|---|---|
| MAA : Acetonitrile | (0.67)(0.90) | (0.265)(0.237) | (0.61)(0.32) + (0.52)(0.07) |
| 2-Vpy(#1) : Acetonitrile | (0.71)(0.90) | (0.613)(0.237) | (0.00)(0.32) + (0.59)(0.07) |
| 2-Vpy(#2) : Acetonitrile | (0.71)(0.90) | (0.613)(0.237) | (0.00)(0.32) + (0.59)(0.07) |
| 2-Vpy(#1) : T1 | (0.71)(1.25) | (0.613)(1.223) | (0.00)(0.43) + (0.59)(0.41) |
| 2-Vpy(#2) : T2 | (0.71)(0.62) | (0.613)(0.210) | (0.00)(0.45) + (0.59)(0.60) |
| MAA:T3 | (0.67)(1.55) | (0.265)(0.400) | (0.61)(1.17) + (0.52)(0.40) |
| Totals based on Equations A1–A3 | 0.49 | 0.631 | 1.20 |

## REFERENCES


1. Narayanan, S.R. and Crane, L.J. (1990) Affinity Chromatography Supports: A Look at Performance Requirements. *Trends Biolotechnol.*, 8: 12–16.
2. Wilchek, M. and Miron, T. (1999) Thirty Years of Affinity Chromatography. *React. Funct. Polym.*, 41: 263–268.
3. Turkova, J. (1999) Oriented Immobilization of Biologically Active Proteins as a Tool for Revealing Protein Interactions and Function. *J. Chromatogr. B*, 722: 11–31.
4. Lakhiari, H., Jozefonvicz, J., and Muller, D. (1998) Influence of The Nature of Coupling Agents on Insulin Adsorption on Supports Grafted with Sialic Acid for High-Performance Affinity Chromatography. *J. Chromatogr. B*, 706: 33–41.
5. Theodoridis, G. and Manesiotis, P. (2002) Selective Solid Phase Extraction Sorbent for Caffeine Made by Molecular Imprinting. *J. Chromatogr. A*, 948: 163–169.
6. Hwang, C. and Lee, W. (2001) Chromatographic Resolution of the Enantiomers of Phenylpropanolamine by Using Molecularly Imprinted Polymer as the Stationary Phase. *J. Chromatogr. B*, 765: 45–53.
7. Surugiu, I., Ye, L., Yilmaz, E., Dzgoev, A., Danielsson, B., Mosbach, K., and Haupt, K. (2000) An Enzyme-Linked Molecularly Imprinted Sorbent Assay. *Analyst*, 125: 13–16.
8. Panasyuk, T.L., Mirsky, V.M., Piletsky, S.A., and Wolfbeis, O.S. (1999) Electropolymerized Molecularly Imprinted Polymers as Receptor Layers in Capacitive Chemical Sensors. *Anal. Chem.*, 71: 4609–4613.
9. Andersson, L. et al. (1996) Molecular Imprinting: The Current Status and Future Development of Polymer-Based Recognition Systems. *Adv. Mol. Cell Biol.*, 15B: 651–670.
10. Haupt, K. and Mosbach, K. (2000) Molecularly Imprinted Polymers and Their Use in Biomimetic Sensors. *Chem. Rev.*, 100: 2495–2504.
11. Sellergen, B. (2001) The non-covalent approach to molecular imprinting. In *Molecularly Imprinted Polymers, Man-Made Mimics of Antibodies and Their Applications in Analytical Chemistry*; Sellergren, Bèorje, Ed.; Elsevier: Tokyo; 113–184.

12. Sellergren, B., Ekberg, B., and Mosbach, K. (1985) Molecular Imprinting of Amino Acid Derivatives in Macroporous Polymers. Demonstration of substrate and enantio-selectivity by chromatographic resolution of racemic mixtures of amino acid derivatives. *J. Chromatogr.*, 347: 1–10.
13. Andersson, L.I. and Mosbach, K. (1990) Enantiomeric Resolution on Molecularly Imprinted Polymers Prepared with only Non-Covalent and Non-Ionic Interactions. *J. Chromatogr.*, 516: 313–322.
14. Dunkin, I.R., Lenfeld, J., and Sherrington, D.C. (1993) Molecular Imprinting of Flat Polycondensed Aromatic Molecules in Macroporous Polymers. *Polymer*, 34: 77–84.
15. Fu, Q., Sanbe, H., Kagawa, C., Kunimoto, K.K., and Haginaka, J. (2003) Uniformly Sized Molecularly Imprinted Polymer for (S)-Nilvadipine. Comparison of Chiral Recognition Ability with HPLC Chiral Stationary Phases Based on a Protein. *Anal. Chem.*, 75: 191–198.
16. Hart, B.R. and Shea, K.J. (2002) Molecular Imprinting for the Recognition of N-Terminal Histidine Peptides in Aqueous Solution. *Macromolecules*, 35: 6192–6201.
17. Ramstrom, L.I., Andersson, K., and Mosbach, K. (1993) Recognition Sites Incorporating Both Pyridinyl and Carboxy Functionalities Prepared by Molecular Imprinting. *J. Org. Chem.*, 58: 7562–7564.
18. Katz, A. and Davis, M.E. (1999) Investigation into The Mechanisms of Molecular Recognition with Imprinted Polymer. *Macromolecules*, 32: 4113–4121.
19. (a) Andersson, H.S.Karlsson, J.G., Piletsky, S.A. Koch-Schmidt, A.C. Mosbach, K. and Nicholls, I.A. (1999) Study of the Nature of Recognition in Molecularly Imprinted Polymers, II [1]: Influence of Monomer–Template Ratio and Sample Load on Retention and Selectivity. *J. Chromatogr. A*, 848: 39–49; (b) Nicholls, I.A., Adbo, K., Andersson, H.S., Andersson, P.O., Ankarloo, J., Hedin-Dahlstrom, J., Jokela, P., Karlsson, J.G., Olofsson, L., Rosengren, J., Shoravi, S., Svenson, J., and Wikman, S. (2001) Can We Rationally Design Molecularly Imprinted Polymers? *Anal. Chim. Acta*, 435: 9–18.
20. Wulff, G., Groß, T., Schönfeld, R., Schrader, T., and Kirsten, C. (1998) Molecular imprinting for the preparation of enzyme-analogous polymers. In *Molecular and Ionic Recognition with Imprinted Polymers*; Bartsch Richard A. and Maeda, Mizuo, Ed.; American Chemical Society: Washington, DC; Chapter 2.
21. Sellergen, B. (2001) Fundamental aspects on the synthesis and characterization of imprinted network polymers. In *Molecularly Imprinted Polymers, Man-Made Mimics of Antibodies and Their Applications in Analytical Chemistry*; Sellergren, Bèorje, Ed.; Elsevier: Tokyo; 21–57.
22. Umpleby, R.J., Baxter, S.C., Chen, Y.Z., Shah, R.N., and Shimizu, K.D. (2001) Characterization of Molecularly Imprinted Polymers with the Langmuir-Freundlich Isotherm. *Anal. Chem.*, 73: 4584–4591.
23. Turiel, E., Perez-Conde, C., and Martin-Esteban, A. (2003) Assessment of the Cross-Reactivity and Binding Sites Characterization of a Propazine-Imprinted Polymer Using the Langmuir-Freundlich Isotherm. *Analyst*, 128: 137–141.
24. Kipling, J.J. (1965) *Adsorption from Solutions of Non-Electrolytes*; Academic Press: New York.
25. O'Shannessy, D.J. (1989) Molecular Imprinting of Amino Acid Derivatives at Low Temperature (0°C) Using Photolytic Homolysis of Azobisnitriles. *Anal. Biochem.*, 177: 144–149.

26. Moller, K., Nilsson, U., and Crescenzi, C. (2001) Synthesis and Evaluation of Molecularly Imprinted Polymers for Extracting Hydrolysis Products of Organophosphate Flame Retardants. *J. Chromatogr. A*, 938: 121–130.
27. Abraham, M.H. (1993) Scales of Solute Hydrogen-Bonding: Their Construction and Application to Physicochemical and Biochemical Processes. *Chem. Soc. Rev.*, 22: 73–83.
28. Abraham, M.H. and Platts, J.A. (2001) Hydrogen Bond Structural Group Constants. *J. Org. Chem.*, 66: 3484–3491.
29. Burleigh, M.C., Dai, S., Hagaman, E.W., and Lin, J.S. (2001) Imprinted Polysilsesquioxanes for the Enhanced Recognition of Metal Ions. *Chem. Mater.*, 13: 2537–2546.
30. Makote, R.D. and Dai, S. (2001) Matrix-Induced Modification of Imprinting Effect for $Cu^{2+}$ Adsorption in Hybrid Silica Matrices. *Anal. Chim. Acta*, 435: 169–175.
31. Yilmaz, E., Mosbach, K., and Haupt, K. (1999) Influence of the Functional and Crosslinking Monomers and the Amount of Template on the Performance of Molecularly Imprinted Polymers in Binding Assays. *Anal. Commun.*, 36: 167–170.
32. Barbosa, J., Fonrodona, G., Marques, I., Buti, S., and Toro, I. (1997) Factor Analysis Applied to the Correlation Between Dissociation Contants and Solvatochromic Parameters in Water-Acetonitrile Mixtures. 1. Solvent Effects on the Dissociation of Carboxylic Acid Groups in Some Diuretics, Quinolones, Buffers and Peptides. *Trends Anal. Chem.*, 16: 104–11.